

STRANGE FILAMENTARY STRUCTURES (“FIREBALLS”) AROUND A MERGER GALAXY IN THE COMA CLUSTER OF GALAXIES¹

MICHITOSHI YOSHIDA², MASAFUMI YAGI³, YUTAKA KOMIYAMA^{3,4}, HISANORI FURUSAWA⁴, NOBUNARI KASHIKAWA³, YUSEI KOYAMA⁵, HITOMI YAMANOI^{3,6}, TAKASHI HATTORI⁴ AND SADANORI OKAMURA^{5,7}

Draft version November 1, 2018

ABSTRACT

We found an unusual complex of narrow blue filaments, bright blue knots, and H α -emitting filaments and clouds, which morphologically resembled a complex of “fireballs,” extending up to 80 kpc south from an E+A galaxy RB199 in the Coma cluster. The galaxy has a highly disturbed morphology indicative of a galaxy–galaxy merger remnant. The narrow blue filaments extend in straight shapes toward the south from the galaxy, and several bright blue knots are located at the southern ends of the filaments. The R_C band absolute magnitudes, half light radii and estimated masses of the bright knots are $\sim -12 - -13$ mag, $\sim 200 - 300$ pc and $\sim 10^{6-7} M_\odot$, respectively. Long, narrow H α -emitting filaments are connected at the south edge of the knots. The average color of the fireballs is $B - R_C \approx 0.5$, which is bluer than RB199 ($B - R = 0.99$), suggesting that most of the stars in the fireballs were formed within several times 10^8 yr. The narrow blue filaments exhibit almost no H α emission. Strong H α and UV emission appear in the bright knots. These characteristics indicate that star formation recently ceased in the blue filaments and now continues in the bright knots. The gas stripped by some mechanism from the disk of RB199 may be traveling in the intergalactic space, forming stars left along its trajectory. The most plausible fireball formation mechanism is ram pressure stripping by high-speed collision between the galaxy and the hot intra-cluster medium. The fireballs may be a snapshot of diffuse intra-cluster population formation, or halo star population formation in a cluster galaxy.

Subject headings: galaxies: clusters: general — galaxies: evolution — galaxies: dwarf — galaxies: kinematics and dynamics — intergalactic medium

1. INTRODUCTION

Clusters of galaxies are ideal experimental laboratories for studying environmental effects on galaxy evolution (e.g. Bosselli & Gavazzi 2006). Cluster galaxy density varies widely from edge to core, the intergalactic space is often filled with X-ray emitting hot gas, and the cluster’s large mass forms a very deep gravitational potential around its center. These properties give us observational means to investigate how galaxy density, ambient gas–galaxy interaction, and strong gravitational drag force affect galaxy evolution.

Several lines of observational evidence suggest that drastic galaxy evolution occurred in clusters of galaxies from the redshift $z \sim 1$ to the present. Early type galaxies form a dominant population in the inner region of local rich clusters, and in particular, S0 galaxies are preferentially found in and around the cluster

core region (Dressler 1980, 1994; Dressler et al. 1997; Postman & Geller 1984; Goto et al. 2003; van der Wel et al. 2007). This relationship—the morphology–density relationship—is also observed at high redshift ($z \sim 1$). However, this enhancement of the fraction of S0 galaxies around a cluster core is less remarkable in high redshift clusters than in local clusters (Smith et al. 2005; Postman et al. 2005). In addition, a higher blue galaxy fraction has been established for high-redshift clusters (Butcher & Oemler 1978, 1984). Furthermore, a rapid rise in the luminosity function (LF) of member galaxies toward the faint end has been reported in several local rich clusters (Popesso et al. 2005; Trentham, Sampson & Banerji 2005; Popesso et al. 2006; Milne et al. 2007; Adami et al. 2007; Yamanoi et al. 2007). However, the LFs of some rich clusters at $z \approx 0.3$ may exhibit no such rapid increase at those faint ends (Harsono & De Propris 2007). These observational facts suggest that in terms of morphology, color, and population, rapid evolution of galaxies occurred in clusters from $z \sim 1$ to the present.

Several environmental effects that explain the evolution of cluster galaxies have been proposed, including galaxy–galaxy interaction (Farouki & Shapiro 1981; Icke 1985), galaxy harassment (Moore et al. 1996), tidal interaction with cluster potential (Henriksen & Byrd 1996), ram pressure stripping (Gunn & Gott 1972; Vollmer et al. 2001; Kronberger et al. 2008), turbulent viscous stripping (Nulsen 1982), and galaxy starvation (Larson, Tinsley & Caldwell 1980; Bekki, Couch & Shioya 2002). In addition, many observational studies have been made to identify the dominant environmental processes in clusters (cf., Bosselli & Gavazzi 2006 and references therein).

¹ Based on data collected at the Subaru Telescope, operated by the National Astronomical Observatory of Japan.

² Okayama Astrophysical Observatory, National Astronomical Observatory, Kamogata, Okayama 719-0232, Japan; yoshida@oao.nao.ac.jp.

³ Optical and Infrared Astronomy Division, National Astronomical Observatory, Mitaka, Tokyo 181-8588, Japan.

⁴ Subaru Telescope, National Astronomical Observatory of Japan, 650 North A’Ohoku Place, Hilo, HI 96720, USA.

⁵ Department of Astronomy, University of Tokyo, Tokyo 113-0033, Japan.

⁶ Department of Astronomical Science, School of Physical Sciences, The Graduate University for Advanced Studies (Sokendai), National Astronomical Observatory of Japan, Tokyo 181-8588, Japan.

⁷ Research Center for the Early Universe, University of Tokyo, Tokyo 113-0033, Japan.

However, the kinds of physical processes that are dominant in rapid galaxy evolution in clusters are still unclear.

Recently, Cortese et al. (2007) (C07) found two peculiar galaxies near the central regions of rich clusters Abell 1689 and Abell 2667 at $z \approx 0.2$. These galaxies have disturbed morphology and are associated with many small blue blobs extending toward one side of the galaxies. These blobs have absolute magnitudes of $M_B \approx -11 - -12$, corresponding to masses of $10^{6-8} M_\odot$. C07 detected [OII] emission from some of the blobs and between the blobs and the host galaxies. The brightness and the size of the blobs are similar to those of dwarf elliptical galaxies or ultracompact dwarf galaxies (Drinkwater et al. 2004). C07 suggested that the phenomena they found may be snapshots of the transformation of spiral galaxies to S0 galaxies, and may give insight into the origin of cluster faint-end populations.

Here we report the discovery of a strange complex of narrow blue filaments and knots extending toward one side of a disturbed E+A galaxy, RB199, in the Coma cluster. New deep optical broadband and narrowband ($H\alpha$) imaging observations of the central region of the Coma cluster revealed this structure. The morphology of the structure is very similar to that of the phenomena reported in C07, and the sizes and the luminosities of the knots in the structure are comparable to C07's blobs. This structure may be a nearby counterpart of C07's phenomena.

We assumed the cosmological parameters ($h_0, \Omega_m, \Omega_\Lambda$) = (0.73, 0.24, 0.72) and the distance modulus of the Coma cluster to be 35.05 (Yagi et al. 2007). The linear scale at the Coma cluster is 474 pc arcsec $^{-1}$ under this assumption.

2. OBSERVATION AND DATA REDUCTION

We observed a 34×27 arcmin region near the Coma cluster center (α, δ) (J2000.) = ($12^h 59^m 26^s$, $+27^\circ 44' 16''$) with Suprime-Cam (Miyazaki et al. 2002) attached to the Subaru Telescope on April 28 and May 3, 2006 and May 13–15, 2007 (Table 1). The main purpose of these observations was to study the faint-end population and star formation in the Coma cluster. We used two broadband filters, B , R_C and a narrowband filter (N-A-L671, hereafter $H\alpha$ NB). The $H\alpha$ NB filter is designed for observing $H\alpha$ -emitting objects in the Coma cluster at $z = 0.0225$, and has a bell-shaped transmission with a central wavelength of 6712 Å and a FWHM of 120 Å.

We reduced the imaging data in the standard manner. Since some data have low S/N because of bad weather, we chose better S/N images to make combined images. Photometric calibration was performed using photometric standard stars observed on May 3, 2006 (Yagi et al. 2007). We corrected Galactic extinction using the extinction calculator provided on the NASA/IPAC Extragalactic Database (NED) Web site. The basic extinction data were obtained from Schlegel, Finkbeiner & Davis (1998). The limiting surface brightness of each band image was estimated from $1-\sigma$ fluctuation of sky background within a 2 arcsec diameter circular aperture. The limiting surface brightness and the PSF sizes of the final images are summarized in Table 1. We subtracted the R_C image from the $H\alpha$ NB image to produce a continuum subtracted $H\alpha$ image (“pure (net) $H\alpha$ image”). We rescaled the R_C image before the subtraction using several field

stars to equalize the mean flux of the stars in the R_C image to that of the $H\alpha$ image. The resultant limiting surface brightness ($1-\sigma$ fluctuation in a $2''$ circular aperture) of the pure $H\alpha$ image is 2.4×10^{-18} erg s $^{-1}$ cm $^{-2}$ arcsec $^{-2}$, if photon noise of object is negligible.

The lengths and distances given in the following sections are all projected. Since the inclination angles with respect to the sky plane of the features that we found are not known, we do not apply any projection correction. The magnitudes are expressed in the Vega system unless otherwise specified.

3. RESULTS

A false color image made with the B (blue), the R_C (green), and the $H\alpha$ NB (red) images around an amorphous galaxy RB199 (J2000.0, $12^h 58^m 43^s$, $+27^\circ 45' 43''$) is shown in Figure 1. The centering error of the three color images is less than 0.1 pixels, corresponding to $0''.02$. The continuum light is not subtracted from the $H\alpha$ NB image in Figure 1. Contour maps of the B image and the R_C image are shown in Figures 2 and 3. Figure 4 shows a grayscale image of the pure $H\alpha$ image. A remarkable complex of blue filaments and blobs and $H\alpha$ -emitting clouds extends toward the south from RB199 (Figures 1 - 4). The overall morphology of the complex resembles a group of fireballs (large meteors) shooting from the galaxy toward the south (see Figure 1). The complex is thus referred to as the “fireballs.” Figure 5 is a $B - R_C$ color map of RB199 and the bright part of the fireballs. We describe the morphological and color characteristics of RB199 and this strange newly observed feature in the following subsections.

3.1. RB199

RB199 is an E+A galaxy whose projected distance from the center of the Coma cluster is about $18'$ corresponding to 0.5 Mpc at the cluster (Poggianti et al. 2004). RB199's amorphous morphology is clearly seen in Figure 6. The stellar system of RB199 is highly disturbed, indicating that this galaxy is a galaxy-galaxy merger remnant. A past merger event probably induced a starburst in the galaxy and now the star formation activity is in its decay phase, i.e., post-starburst phase. E+A characteristics of the spectrum of the galaxy (Poggianti et al. 2004) suggest that massive OB stars have already died, whereas A-type stars are still alive. The $H\alpha$ absorption dominant post-starburst region is distributed around the nucleus of RB199 as shown in the pure $H\alpha$ image (see Figure 4).

The main structure of RB199 can be divided into two parts: a central disturbed bright “ellipse” and a smooth “disk” extending west of the ellipse (Figure 6). The position angles of the ellipse and the disk are 70° and -70° , respectively.

The $B - R$ color of RB199 within a $163''$ aperture diameter is $B - R = 0.99$ (Poggianti et al. 2004). Our $B - R_C$ color map (Figure 5) reveals a complex inner structure of color distribution in the galaxy. The central ellipse is bluer than the disk. The central blue region in the central ellipse has a thick V-shaped structure and a $B - R_C$ color of $\approx 0.8 - 0.9$. The blue V-shaped structure is surrounded by slightly redder components whose $B - R_C$ color and position angle are ≈ 1.0 and $\approx 70^\circ$, respectively. The disk has a $B - R_C$ color of ≈ 1.2 . Color

distribution of the disk is smooth and no clear color gradient appears.

These characteristics suggest that a past merger concentrated the gas and stars of the progenitor galaxies into the bottom of the gravitational potential of the system and induced a starburst. Some of the newly formed stars from the merging process might have mixed with the preexisting disk stars and formed the disk of RB199.

3.2. The fireballs

3.2.1. Morphology

The most striking feature around RB199 is a complex of strange faint blue knots and filaments and H α -emitting ionized gas clouds extending toward the south from the galaxy (the “fireballs”: Figures 1 - 4). The whole structure of the fireballs is schematically drawn in Figure 7. We labeled several characteristic features in the fireballs, such as bright knots, remarkable filaments, and extended faint clouds, as “knot 1,” “filament 1,” “cloud 1,” and so forth (Figure 7). The enlarged false-color images of knots 1 to 5 are shown in Figure 8.

The bright knots are located at the end of the bright blue filaments; for example, knot 1 is located at the southern end of filament 1. Strong H α emission appears at the south sides of the bright knots. Figures 8 and 9 clearly show this configuration. The intensity peaks of the H α emission are slightly displaced to the south of the B band intensity peaks of the bright knots (see Figures 8 and 9).

The blue filaments (filament 1–filament 5) consist of several filaments with narrow, long, straight, or slightly curved shapes, and lengths of ~ 10 – 30 kpc. The roots of the filaments appear to be connected to the central ellipse of RB199 (Figure 1, see also Figure 7). The most prominent filament is filament 1. It extends linearly toward knot 1, which is the brightest knot in the blue filaments, and connects to filament 2 at the west side of knot 1. Filament 3 contains two straight parallel filaments extending outward from the central ellipse. Filament 4 ends at knot 3 and knot 4. Knot 4 is bright in H α emission and is smoothly connected to the most remarkable H α feature, H α filament 1. H α filament 1 has a linear, slightly wiggled morphology with a length of ≈ 15 kpc and a width of ≈ 2 kpc.

The bright knots are spatially resolved. Their sizes, measured at B band surface brightness of $28 \text{ mag arcsec}^{-2}$, are ~ 1 – 2 kpc (Table 2). To estimate the half light radii (the effective radii, r_e) of the knots, we fitted Gaussian profiles blurred by the point spread function (PSF) to the light profiles of the knots. Then we derived r_e using the relation $r_e \approx 1.18 \sigma$. The r_e of the knots are ≈ 200 – 300 pc. Although the light distributions of the knots are unlikely to exhibit Gaussian profiles, the light profiles of the knots, in particular knots 1, 2, and 5, are well represented with Gaussians. Thus, the r_e are good approximations of the knot sizes.

About 50 kpc from RB199 (Figure 1) is a faint, diffuse filament. This filament, filament 5, is slightly displaced to the east from the line connecting filaments 3, 4, and H α filament 1 (see also Figure 7). Filament 5 is marginally detected in R_C band, indicating that it is very blue. In addition, at the east and west of an elliptical galaxy G5 (located about 80 kpc from RB199) are

faint, diffuse H α clouds (Figure 1). They are very faint, but are marginally seen in the pure H α image (Figure 4). They are also observed as faint red diffuse clouds in Figure 1.

3.2.2. Optical photometry

The results of the photometry of the fireballs are summarized in Table 2. The bright continuum knots have absolute magnitudes of $M_B \sim -12$ and $M_R \sim -12$ – -13 . The typical r_e is ≈ 200 – 300 pc (see section 3.2.1). These values are similar to those of faint dwarf ellipticals in the Virgo cluster (e.g., Ichikawa et al. 1990) or the faint ends of local dwarf galaxies (Belokurov et al. 2007). Assuming a mass to luminosity ratio $M/L_R = 1$ for these knots, their masses are $\sim 10^{6-7} M_\odot$. The mean color of the blue filaments are $B - R_C \approx 0.5$, corresponding to early F stars in the main sequence. The H α luminosities of the bright knots are on the order of $10^{38} \text{ erg s}^{-1}$. We did not apply flux correction of possible contamination of [NII] $\lambda\lambda 6548/6583$ emission for the H α photometry. Thus, the H α fluxes and luminosities in Table 2 are upper limits, possibly decreased by a few tens % due to [NII] contamination. This uncertainty, however, does not affect the following discussion. Assuming that all the H α emission comes from star-forming regions, and using the $L_{\text{H}\alpha}$ to star formation rate (SFR) conversion relationship by Kennicutt (1998), we found that the corresponding SFRs of the knots are on the order of $10^{-3} M_\odot \text{ yr}^{-1}$ (Table 2). The internal reddening correction was not applied in this calculation.

The fireballs are much bluer than any region of RB199 (Figure 5). This suggests that the stellar population or the dust contents of the fireballs is different from those of the galaxy disk. Figure 10 shows the color distribution in the fireballs. The filaments clearly grow bluer with distance from the nucleus of RB199. This means either that the stellar population becomes younger farther out from the galaxy, or that the filaments become dustier at shorter distances.

3.2.3. Ultraviolet data

To investigate star formation activity in the fireballs, we downloaded UV images around RB199 from the Web site of the second data release of Galaxy Evolution Explorer (GALEX) Nearby Galaxy Survey⁸ (Martin et al. 2005). The FUV ($\lambda\lambda 1344 - 1786\text{\AA}$) and NUV ($\lambda\lambda 1771 - 2831\text{\AA}$) contour maps are superposed on the grayscale B band image in Figures 11 and 12.

Note that most of the bright knots in the fireballs are bright in both the FUV and NUV bands. Knots 1–5 are clearly visible both in the FUV and NUV images. In contrast, knot 6 can be seen only in the FUV image. Filaments 1 and 3 are also visible in the NUV image. In addition, very faint features are marginally detected in both FUV and NUV images at the position of filament 5 (Figures 11 and 12).

The UV magnitudes listed on the GALEX Web site and the FUV – B colors in the AB system for the bright knots are summarized in Table 3. All the bright knots are detected in the FUV band. Although knot 5 is visible in the NUV image (Figure 12), the NUV magnitude is

⁸ <http://galex.stsci.edu/GR2/>

not listed on the Web site. We thus measured the NUV magnitude of knot 5 directly from the NUV image, calibrating using the magnitude of knot 1. We also obtained the NUV magnitudes of filaments 1 and 3 in the NUV image (Table 3).

Knot 1 and 2 have FUV magnitudes of ≈ 21.5 and the FUV – NUV colors of these knots are almost flat. Knot 3 + 4 is about one magnitude fainter than knots 1 and 2 in the NUV, and slightly redder. Knot 5 and 6 are almost two magnitudes fainter than knots 1 and 2 in the FUV band. Using the conversion formula from FUV and NUV magnitudes to SFR by Iglesias-Paramo et al. (2006), we derived the SFRs of knots 1–3 as $\sim 2 - 5 \times 10^{-3} M_{\odot} \text{ yr}^{-1}$ from the FUV magnitudes and $\sim 6 - 10 \times 10^{-3} M_{\odot} \text{ yr}^{-1}$ from the NUV magnitudes. These values are somewhat larger than, but still consistent with, the SFRs derived from H α luminosities (see Table 2).

Note that the FUV – B colors of the bright knots are all very blue, $-0.5 - -0.9$, indicating that active star formation occurs in the knots. These blue colors and the strong H α emission seen at the southern sides of the bright knots strongly support the argument that the knots are current star-forming sites. Comparison of the optical-UV colors of the fireballs with color evolution models of star-forming galaxies is made in the next section.

3.2.4. Comparison of the colors with star-formation models

To estimate the age of the filaments, we compared their colors with model calculations of color evolution of star-forming stellar systems using PEGASE Ver.2 (Fioc & Rocca-Volmerange 1997). We assumed that the initial mass function (IMF) follows the Salpeter IMF from $0.1 M_{\odot}$ to $120 M_{\odot}$. Initial metallicity is $0.2 Z_{\odot}$ in this calculation. Dust extinction was not included in our calculations. We derived color evolutions for four cases: constant star formation (“CS” model), exponentially decaying star formation with a decay timescale of 100 Myr (“E100” model), 200 Myr (“E200” model), and 300 Myr (“E300” model).

Figures 13 and 14 show a color–color diagram of the $B - R_C$ to FUV – B , $B - R_C$ to FUV – B , respectively. All the colors of the bright knots are consistent with the E200 model or the E300 model with an age of several times 10^8 yr to 1 Gyr (Figures 13 and 14). Figure 14 also shows that the colors of the blue filaments close to the galaxy (filaments 1 and 3) are somewhat older than the bright knots, and are consistent with the E300 model with an age older than 1 Gyr, or the E200 model with an age of 1 Gyr. Dust extinction trends are shown as arrows at the right-bottom corners of Figures 13 and Figure 14. We derived the extinction trends using the reddening curve of star-forming galaxies proposed by Calzetti et al. (2000). In both figures, the extinction trends almost follow the model loci along the age sequence. If dust extinction is present in the knots, their predicted ages are much younger; in other words, the ages estimated with Figures 13 and 14 are the maximum values for the knots. We thus conclude that the average maximum age of the bright knots is several times 10^8 yr, and the maximum ages of the blue filaments that are located closer than the knots to the galaxy are around 1 Gyr.

Although we have no UV data for the other filaments of the fireballs, we roughly estimate their ages using optical

$B - R_C$ color only. Using the E300 model, the ages of ~ 700 Myr, ~ 1.2 Gyr, and ~ 500 Myr are estimated for filament 2, filament 4, and H α filament 1, respectively, in the case of no dust extinction. The most distant blue filament, filament 5, is very blue, and its age is estimated to be much younger than 500 Myr. In conclusion, the maximum age of the filaments within 20 kpc from the galaxy is ~ 1 Gyr, that of the knots at 20–40 kpc from the galaxy is $\sim 500 - 1000$ Myr, and that of the farthest filaments is ≤ 500 Myr.

This age gradient indicates that the stellar components of the fireballs would be formed after the stripping event. In other words, the gas stripped by some mechanism from the disk of RB199 travels in the intergalactic space, forming stars and leaving the formed stars along its trajectory. This hypothesis is supported by the spatial distribution of the H α emission and the bright knots. The bright H α clouds are located at the southern edges of the bright knots and almost no H α emission is observed in the blue filaments. This indicates that active star formation is now ongoing at the far end of the blue filaments. The hypothesis may also be supported by the fact that the ages of the filaments and knots are roughly consistent with the travel time from the galaxy to the edge of the fireballs ($\sim 60 - 80$ kpc), assuming that the outflow velocity of the stripped material is on the order of 10^2 km s^{-1} . Although the velocities of the filaments and the knots are not known, outflow velocities of an order of 10^2 km s^{-1} were observed in similar stripping phenomena (e.g. Yoshida et al. 2004; Cortese et al. 2006; Yagi et al. 2007).

The color gradient in the blue filaments could also be interpreted as due to dust absorption. If this is the case, the above discussion of age gradient loses its meaning. However, the stellar population of the fireballs is certainly very young because dust absorption correction makes the true colors of the fireballs bluer than the observed ones (see Figures 13 and 14), which strengthens the premise that the stars were formed very recently.

4. FORMATION MECHANISM OF THE FIREBALLS

The newly found strange feature, the “fireballs,” around RB199 is extended in one direction from the galaxy as a group of narrow blue filaments and bright knots with which H α and UV emission are associated. Here we discuss possible fireball formation mechanisms.

C07 found many small blobs extending to one side of galaxies near the cores of two $z \approx 0.2$ rich clusters in the course of a cluster survey with *Hubble Space Telescope* Advanced Camera for Survey. Sun, Donahue & Voit (2007) also reported many star-forming blobs distributed around a very long X-ray/H α tail of a galaxy in the nearby rich cluster Abell 3627. The blobs found by C07 are distributed in faint optical filaments (C07). They detected [OII] emission around some of the blobs, which indicates that star formation is under way in and around the blobs. The morphology and colors of the blobs and the filaments found by C07 are very similar to the fireballs of RB199. They argued that tidal stripping by interaction between deep cluster gravitational potential and/or ram pressure stripping by high-speed collision between the galaxies and the intra-cluster medium (ICM) are responsible for forming the strange blobs they found. Following C07, we examine the above two processes for

validity as the formation mechanism of the fireballs.

4.1. Tidal stripping

Tidal forces induced by galaxy–galaxy interaction disrupt the stellar disks and often throw stars far from the galaxies. Since RB199 appears to be a merger, it is natural to interpret the fireballs as tidal tails formed by tidal force induced by the merging process. The morphology of the fireballs is, however, very strange compared to other merger tidal tails such as NGC 4038/39 (Schweizer 1978), NGC 7252 (Hibbard & van Gorkom 1996), Arp299 (Hibbard & Yun 1999), and IRAS 19254–7245 (Mirabel, Lutz & Maza 1991). In many cases, tidal tails of merging galaxies have long smooth morphologies extending in one or two directions from the merger main body (Hibbard & van Gorkom 1996). The disrupted, multiple filamentary, “splash”-like morphology of the fireballs of RB199 is very rare and peculiar. Thus, from a morphological point of view, it is unlikely that a past merging event is responsible for forming the fireballs, although we can not rule out some special situation or conditions during the merger that produced such peculiar tidal features.

Tidal forces induced by interactions between RB199 and its nearby galaxies may strip the disk gas and stars of RB199 and may form the fireballs. In fact, several galaxies appear in the vicinity of RB199 (G1–G4 in Figure 2). Among these galaxies, G1 has a radial velocity of 6665 km s^{-1} (Colless & Dunn 1996), indicating that this galaxy is a Coma member. However, no tidal features—bridges, tails, ripples, and so on—appear around G1. Those features are also not found around G2–G4. Another candidate galaxy that can strip the disk gas of RB199 is the galaxy about 80 kpc south of RB199 (G5 in Figure 2). This galaxy is located in the extension line of the fireballs, but the morphology of this galaxy exhibits no sign of strong tidal disturbances. To strip the outer disk of a galaxy through tidal forces in close encounters with other galaxies, without disturbing the perturbing galaxies, the perturbers must be more massive than the mass of the perturbed galaxy. All of the above mentioned galaxies are, however, much fainter than RB199, meaning that these galaxies are less massive than RB199. Furthermore, the colors of G2, G3, and G4 are significantly redder than the average color of Coma ellipticals, indicating that these are background galaxies. In fact, the photometric redshifts of these galaxies determined by the SDSS project are $\sim 0.3 - 0.4$. Therefore, it is not plausible that these galaxies significantly perturbed RB199 in the past.

The deep gravitational potential of a rich cluster of galaxies exerts strong tidal forces on galaxies crossing its core region. When a galaxy crosses a cluster core region, if the radial acceleration by the cluster gravity exceeds the centrifugal acceleration of the crossing galaxy, the outer part of the galaxy is stripped by the tidal force of the cluster (C07). The radial acceleration a_c by a cluster core whose mass within r is M_c is written as

$$a_c = GM_c \left[\frac{1}{r^2} - \frac{1}{(r+R)^2} \right], \quad (1)$$

where R is the radius of the crossing galaxy and r is the distance between the galaxy and the cluster center. The

centrifugal acceleration of the galaxy is written as

$$a_{\text{gal}} = G \frac{M_{\text{gal}}}{R^2}, \quad (2)$$

where M_{gal} is the mass of the galaxy. The projected distance from the center of the Coma cluster and RB199 is $\approx 0.5 \text{ Mpc}$. The total (stars + gas + dark matter) mass of the Coma cluster within the radius of 0.5 Mpc was estimated as $\approx 3 \times 10^{14} M_{\odot}$ (Lokas & Mamon 2003). The R band luminosity of RB199 is $1.4 \times 10^9 L_{\odot}$ (Mobasher et al. 2001). Thus, assuming $M/L_R \sim 2 - 3$, which is a typical value of disk M/L ratios for nearby spiral galaxies (Forbes 1992; Palunas & Williams 2000; Yoshino & Ichikawa. 2008), the mass of the disk of RB199 is calculated as $3 - 4 \times 10^9 M_{\odot}$. The roots of the blue filaments are all connected to the central ellipse of RB199; thus, the effective radius of the disturbed region of the galaxy is that of the ellipse, i.e., $R \sim 5 \text{ kpc}$. With these values, one can surmise that a_{gal} is one order of magnitude larger than a_c . This means that the cluster potential can hardly strip the outer disk component of RB199. Even if the M/L_R of the galaxy is almost unity, a_{gal} is still larger than a_c . Therefore, tidal stripping by cluster–galaxy interaction is not a possible candidate for a formation mechanism of the fireballs around RB199.

4.2. Ram pressure stripping

When a gas-rich disk galaxy collides with the hot ICM at high speed ($v \sim 10^3 \text{ km s}^{-1}$), ram pressure from the ICM strips massive amounts of gas from the galaxy. This process, ram pressure stripping, has been discussed in many studies as an efficient gas removing mechanism for galaxies in clusters (Gunn & Gott 1972; Abadi, Moore & Bower 1999; Fujita & Nagashima 1999; Vollmer et al. 2001; Schulz & Struck 2001; Bekki & Couch 2003; Roediger & Brüggen 2007). From an observational point of view, Cayatte et al. (1990, 1994) found that HI gas is significantly deficient for spiral galaxies in the core region of the Virgo cluster. Bravo-Alfaro et al. (2000, 2001) found strong HI deficiency for bright spiral galaxies inside a radius of 0.6 Mpc from the center of the Coma cluster. In addition, detailed case studies have been carried out for many objects through optical and radio observations (NGC 4388: Yoshida et al. 2002, 2004; Vollmer & Huchtmeier 2003; Oosterloo & van Gorkom 2005; NGC 4402: Crawl et al. 2005; NGC 4438: Chemin et al. 2005; NGC 4522: Kenny & Koopmann 1999; Vollmer et al. 2004).

The position and the velocity of RB199 suggest that the galaxy suffers strong ram pressure from the ICM through high-speed collision with it. RB199 is located at the edge of the dense ICM associated with the main body of the Coma cluster (Poggianti et al. 2004). In addition, the radial velocity of RB199 ($v \approx 8700 \text{ km s}^{-1}$; Mobasher et al. 2001) is quite large with respect to the mean radial velocity of the Coma cluster ($v \approx 6500 \text{ km s}^{-1}$). To determine whether the disk gas of RB199 can be stripped, we try to estimate the ram pressure stripping radius R_{strip} for the RB199 case. When the distribution of stars and gas of the galaxy disk is a double exponential, R_{strip} is estimated as

$$R_{\text{strip}} = 0.5 R_0 \times \ln \left[\frac{GM_{\text{star}} M_{\text{gas}}}{v^2 \rho_{\text{ICM}} 2\pi R_0^4} \right], \quad (3)$$

where M_{star} and M_{gas} are the mass of the stars and the gas in the galaxy disk, respectively, v is the galaxy velocity relative to the ICM, ρ_{ICM} is the density of the ICM, and R_0 is the radial scale length of the disk (Domainko et al. 2006). Substituting $4.2 \times 10^9 M_{\odot}$, $\sim 10^8 M_{\odot}$, $\sim 10^{-4} \text{ cm}^{-3}$ and $\sim 2000 \text{ km s}^{-1}$ for M_{star} , M_{gas} , ρ_{ICM} and v , respectively, we obtain

$$R_{\text{strip}} = 0.5 \left(\frac{R_0}{\text{kpc}} \right) \times \ln \left[25.4 \times \left(\frac{R_0}{\text{kpc}} \right)^{-4} \right]. \quad (4)$$

We fitted an exponential disk function to the light profile of the central ellipse of RB199 along PA=70° and found that $R_0 \approx 1.5 \text{ kpc}$. Note that RB199 has an irregular shape and does not have a clear exponential disk. Hence the R_0 we derived above is not a correct “effective radius.” This R_0 is, however, an indicator of the surface density distribution of the galaxy, and thus is useful for determining whether the disk gas of RB199 can be stripped by the ram pressure of the ICM. With this value, we derived $R_{\text{strip}} \approx 1.2 \text{ kpc}$. This means that almost all the gas in the disk of RB199 would be stripped by the ram pressure of the ICM.

The morphology of the fireballs also supports the ram pressure stripping hypothesis. The fireballs extend from one side of RB199, and ram pressure stripping forms a filamentary structure extending on one side from the colliding galaxy (Abadi et al. 1999; Quilis, Moor & Bower 2000; Roediger & Hensler 2005; Kronberger et al. 2008). In addition, the configuration in which the ionized gas is far more extended than the stars (the blue filaments and the bright knots) is naturally explained by ram pressure. The gas clouds undergo the ram pressure of the ICM and are accelerated by it continuously after the stripping, whereas the stars are not affected by the ram pressure and suffer the gravitational force of the galaxy. Hence the gas clouds stretch far away from the galaxy while the stars remain relatively nearby. Therefore, we propose that ram pressure stripping is the primary formation mechanism of the fireballs.

A major argument against the ram pressure stripping hypothesis is the fact that the blue filaments and the bright knots of the fireballs consist mainly of stars. Ram pressure stripping can remove only gas from a galaxy and cannot greatly affect the stellar system of the galaxy. Stars are too massive, and their collisional cross sections are too small, to respond to drag force from the ram pressure of the ICM flow. However, note that the stellar population of the fireballs is very young and must largely have been formed after stripping from the host galaxy. In other words, only the gas in the disk was stripped in the initial phase, and the stars were then formed in the stripped gas.

Sun et al. (2007) also argued that the blue blobs they found may have been formed in the stripped gas by the ram pressure. Recently, Kronberger et al. (2008) performed numerical simulations focusing on star formation due to ram pressure stripping and found that strong star formation is triggered in the central region of their model galaxy as well as in the stripped gas filaments behind the galaxy. The star formation blobs, whose sizes and masses are of an order of 1 kpc and $10^7 M_{\odot}$, respectively, extended up to 100 kpc from the galaxy (Kronberger et al. 2008). In their simulations, the stripped

gas filaments have narrow and slightly wiggled straight shapes, whereas the newly formed stars form somewhat diffuse wide filaments. Note that the mass and size of the blobs and the morphology of the complex of the blobs and the filaments derived in the simulations of Kronberger et al. (2008) strongly resemble those of the fireballs we found around RB199. Accordingly, Kronberger et al.’s results strongly support the hypothesis that the fireballs are formed by ram pressure stripping.

In the case that ram pressure stripping is the primary fireball formation driver, the stripped neutral hydrogen (HI) gas would be observed around RB199. Bravo-Alfaro et al. (2000, 2001) made deep HI observations of the Coma cluster using the VLA. RB199 and its surrounding area were within the observation areas of fields 7 and 10 in their study (Bravo-Alfaro et al. 2000). They observed no sign of HI gas around RB199. The primary cause for this is that the recession velocity of RB199 ($\approx 8700 \text{ km s}^{-1}$) is far outside the frequency bands (6.25 MHz) of their observations, which were centered at radial velocities of 5500 km s^{-1} (“field 7”) and 7300 km s^{-1} (“field 10”) (Bravo-Alfaro et al. 2000).

4.3. Ram pressure stripping with galaxy–galaxy merger

The morphology of RB199 indicates that this galaxy is a merger remnant. We are thus led to the idea that a galaxy–galaxy merger in addition to ram pressure of the ICM may have played an important role in efficiently stripping the gas from RB199. A galaxy–galaxy merger perturbs the interstellar gas in the galaxy disk significantly, and some portion of the gas would flare up above the disk. A combination of this effect and the ram pressure may make gas stripping from the galaxy very efficient. Struck & Brown (2004) performed numerical simulations of ram pressure stripping for merging galaxies infalling to a cluster. Their results support that the above simple picture is correct in principle. They found that strongly interacting galaxy pairs tend to be stripped of much more gas than isolated galaxies by the ram pressure of the ICM (Struck & Brown 2004). This process may be very efficient in stripping the interstellar medium from a galaxy disk, and may strip heavy elements other than HI gas, such as metals, molecules, or dust that make star formation in the stripped gas possible.

One of the most striking features formed by a combination of galaxy–galaxy interaction and ram pressure stripping ever found is the Blue Infalling Group (BIG) in Abell 1367 (Sakai et al. 2002; Gavazzi et al. 2003; Cortese et al. 2006). Very extended ionized gas filaments and blue tails are observed in BIG (Cortese et al. 2006). In addition, many star-forming dwarf galaxies are distributed in BIG (Sakai et al. 2002). Cortese et al. (2006) concluded that the combined action of tidal forces among the galaxies and ram pressure by the ICM produced that peculiar structure. Although BIG is much larger and more luminous than the fireballs around RB199, the phenomena appear similar. In addition, the host galaxies of the blobs of C07 and Sun et al. (2007) have disturbed morphologies, suggesting a past merger. These observational results support the idea that a galaxy–galaxy interaction/merger in addition to ram pressure stripping may make a significant contribution to the formation of fireballs and similar objects.

In conclusion, ram pressure stripping is the key driver

in fireball formation. A galaxy–galaxy merger in addition to the ram pressure may make a considerable contribution to their formation. Tidal interactions between RB199 and the gravitational potential of the Coma cluster would not be strong enough to play a major role in formation of the fireballs.

5. SUMMARY

We found a strange complex (the “fireballs”) of blue filaments and $H\alpha$ clouds that extends up to 80 kpc toward the south from the merging galaxy RB199 in the Coma cluster. The narrow blue filaments are extended in straight shapes and several bright blue knots are located at the south end of the blue filaments. Strong $H\alpha$ emission is associated with the knots. In addition, faint, narrow $H\alpha$ -emitting filaments extend farther from the southern edge of the knots.

The total B and R_C magnitudes of the fireballs are 19.87 and 19.33, respectively. The luminosities of the $H\alpha$ emission associated with the bright knots are $1 - 6 \times 10^{38}$ erg s $^{-1}$, which correspond to a star-formation rate of $\sim 10^{-3} M_\odot$ yr $^{-1}$, assuming all the $H\alpha$ comes from star-forming activity. The average color of the fireballs is $B - R_C \approx 0.5$, which is bluer than RB199 ($B - R_C = 0.99$), and the blue filaments and the bright knots grow bluer with distance from the nucleus of the galaxy. These observational facts suggest that the stars of which the fireballs are composed were formed within several times 10^8 yr and that the stellar population grows younger farther from the galaxy.

Almost no $H\alpha$ emission is observed in the blue filaments but strong $H\alpha$ and UV emissions are associated with the bright knots. These characteristics indicate that star formation has already ceased in the blue filaments and is now in progress in the bright knots. The gas stripped by some mechanism from the disk of RB199 may be traveling in the intergalactic space, forming stars and leaving the formed stars along its trajectories. The R_C -band absolute magnitudes, the half light radii, and the estimated masses of bright knots in the fireballs are $\sim -12 - -13$ mag, $\sim 200 - 300$ pc and $\sim 10^{6-7} M_\odot$, respectively. These values are similar to those of faint dwarf spheroidals in the Virgo cluster or the faint end of local dwarf galaxies. This suggests that the bright knots are gravitationally self-bound systems.

The most plausible formation mechanism of the fireballs is ram pressure stripping by the hot ICM. Tidal stripping by galaxy–galaxy interaction or galaxy–cluster interaction would not be a primary mechanism for the formation of the fireballs. A galaxy–galaxy merger, however, is probably important to make subsequent ram pressure stripping of the ICM more effective in forming this strange structure.

Although whether the stars in the fireballs are all gravitationally bound to RB199 is not known, some structures close to the galaxy may fall back to the galaxy

in the future, oscillating between the two sides of the galaxy disk and eventually forming the halo star population of RB199. Some part of the fireballs may be stripped from RB199 in the future by tidal interaction with nearby galaxies or the cluster gravitational potential, even if they are currently bound to the galaxy. If this is the case, the stripped stars may form a diffuse intra-cluster population (Gregg & West 1998; Okamura et al. 2002; Murante et al. 2004; Krick, Bernstein & Pimbblet 2006; Gerhard et al. 2007).

The fireballs we found in the Coma cluster resemble the compact young blobs found by C07 and Sun et al. (2007) around some cluster galaxies. C07 argued that formation of these compact blobs is rather rare in clusters at $z \approx 0.2$. They found only two examples out of 130 cluster spiral galaxies at $z \approx 0.2$. They also predicted that these features would be more remarkable at $z \geq 0.2$ because the galaxy infalling rate and the gas content of each galaxy are higher in high- z clusters than in local clusters. However, our findings show that formation of compact stellar systems like C07’s blobs around cluster galaxies is still ongoing in the local universe. The Coma cluster has a large substructure of the ICM and a group of galaxies associated with this substructure, indicating that this cluster itself is a merging system (Colless & Dunn 1996). RB199 is located near the border between the main body and the substructure of the ICM (Poggianti et al. 2004). The special conditions of the Coma cluster and RB199 may produce a special environment around RB199, namely, high-ensity ambient gas, high-speed infall, and/or frequent galaxy–galaxy interactions

We thank the staff of the Subaru telescope for their kind help with the observations. This work was carried out in part using data obtained by a collaborative study on the Coma cluster. We thank our collaborators in this study, David Carter, Alister Graham, Shardha Jogee, Neal Miller, and Bahram Mobasher, for their encouragement and helpful comments. We also thank Ikuru Iwata for his help in calculating the color evolution model of a star-forming galaxy. We are grateful to the anonymous referee for constructive suggestions that helped to greatly improve the manuscript. This study was in part carried out using the facilities at the Astronomy Data Center (ADC), National Astronomical Observatory of Japan. This research made use of NASA’s Astrophysics Data System Abstract Service, NASA/IPAC Extragalactic Database, and GALEX Release 2 database. We thank the National Institute of Information and Communications Technology for their support on the high-speed network connection for data transfer and analysis. This work was financially supported in part by a Grant-in-Aid for Scientific Research (B) No.18340055 from the Japan Society for the Promotion of Science (JSPS).

REFERENCES

- Abadi, M. G., Moore, B., & Bower, R. G. 1999, *MNRAS*, 308, 947
- Adami, C., et al. 2007, *A&A*, 472, 749
- Bekki, K., & Couch, W. J. 2003, *ApJ*, 596, L13
- Bekki, K., Couch, W. J., & Shioya, Y. 2002, *ApJ*, 577, 651
- Belokurov, V., et al. 2007, *ApJ*, 654, 897
- Boselli, A., & Gavazzi, G. 2006, *PASP*, 118, 517
- Bravo-Alfaro, H., Cayatte, V., van Gorkom, J. H., & Balkowski, C. 2000, *AJ*, 119, 580
- Bravo-Alfaro, H., Cayatte, V., van Gorkom, J. H., & Balkowski, C. 2001, *A&A*, 379, 347
- Butcher, H., & Oemler, A. 1978, *ApJ*, 219, 18
- Butcher, H., & Oemler, A. 1984, *ApJ*, 285, 426
- Calzetti, D. et al. 2000, *ApJ*, 533, 682

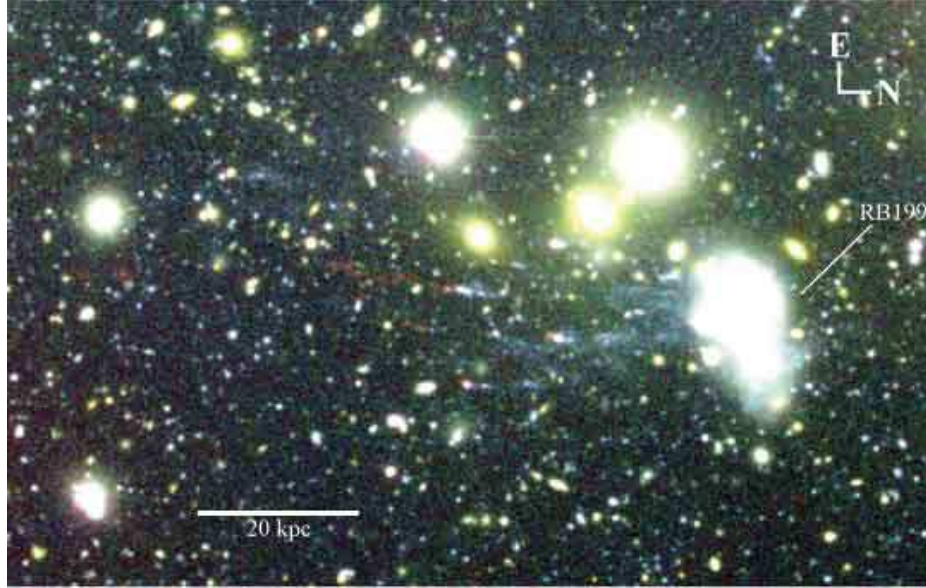


FIG. 1.— False color (B band: blue, R_C band: green, $H\alpha$ NB: red) image of area around RB199. North is right and east is top. RB199 is located at the right side of the image.

- Cayatte, V., van Gorkom, J. H., Balkowski, C., & Kotanyi, C. 1990, *AJ*, 100, 604
- Cayatte, V., Kotanyi, C., Balkowski, C., & van Gorkom, J. H. 1994, *AJ*, 107, 1003
- Chemin, L., et al. 2005, *A&A*, 436, 469
- Colless, M., & Dunn, A. M. 1996, *ApJ*, 458, 435
- Conselice, C. J., & Gallagher, J. S. 1998, *MNRAS*, 297, L34
- Cortese, L., et al. 2006, *A&A*, 453, 847
- Cortese, L., et al. 2007, *MNRAS*, 376, 157 (C07)
- Crowl, H. H., Kenney, J. D. P., van Gorkom, J. H., & Vollmer, B. 2005, *ApJ*, 130, 65
- Domainko, W., et al. 2006, *A&A*, 452, 795
- Dressler, A. 1980, *ApJ*, 236, 351
- Dressler, A. 1994, *ApJ*, 430, 107
- Dressler, A., et al. 1997, *ApJ*, 490, 577
- Drinkwater, M. J., et al. 2004, *PASA*, 21, 375
- Evstigneeva, E. A., Gregg, M. D., Drinkwater, M. J., & Hilker, M. 2007, *AJ*, 133, 1722
- Farouki, R., & Shapiro, S. L. 1981, *ApJ*, 243, 32
- Fioc, M., & Rocca-Volmerange, B. 1997, *A&A*, 326, 950
- Forbes, D. A. 1992, *A&AS*, 92, 583
- Fujita, Y., & Nagashima, M. 1999, *ApJ*, 516, 619.
- Gavazzi, G., et al. 2003, *ApJ*, 597, 210
- Gerhard, O., et al. 2007, *A&A*, 468, 815-822
- Goto, T., et al. 2003, *MNRAS*, 346, 601
- Gregg, M. D., & West, M. J. 1998, *Nature*, 396, 549
- Gunn, J. E., & Gott, J. R. 1972, *ApJ*, 176, 1
- Harsono, D., & De Propris, R. 2007, *MNRAS*, 380, 1036
- Henriksen, M., & Byrd, G. 1996, *ApJ*, 459, 82
- Hibbard, J. E., & van Gorkom, J. H. 1996, *AJ*, 111, 655
- Hibbard, J. E., & Yun, M. S. 1999, *AJ*, 118, 162
- Hilker, M., et al. 2007, *A&A*, 463, 119
- Icke, V. 1985, *A&A*, 144, 115
- Iglesias-Paramo, J., et al. 2006, *ApJS*, 164, 38
- Jáchym, P. et al. 2007, *A&A*, 472, 5
- Kennicutt, R. C. 1998, *ApJ*, 498, 541
- Kenny, J. D. P., & Koopmann, R. A. 1999, *AJ*, 117, 181
- Krick, J. E., Bernstein, R. A., & Pimblet, K. A. 2006, *AJ*, 131, 168
- Kronberger, T., Kapferer, W., Ferrari, C., Unterguggenberger, S., & Schindler, S. 2008, *A&A*, 481, 337
- Larson, R. B., Tinsley, B. M., & Caldwell, C. N. 1980, *ApJ*, 237, 692
- Lokas, E. L., & Mamon, G. A. 2003, *MNRAS*, 343, 401
- Martin, D. C., et al. 2005, *ApJ*, 619, L1
- Milne, M. L., et al. 2007, *AJ*, 133, 177
- Mirabel, I. F., Lutz, D., & Maza, J. 1991, *A&A*, 243, 367
- Miyazaki, S., et al. 2002, *PASJ*, 54, 833
- Mobasher, B., et al. 2001, *ApJS*, 137, 279
- Moore, B., Katz, N., Lake, G., Dressler, A., & Oemler, A. 1996, *Nature*, 379, 613
- Murante, G., et al. 2004, *ApJ*, 607, L83
- Nulsen, P. E. J. 1982, *MNRAS*, 198, 1007
- Okamura, S., et al. 2002, *PASJ*, 54, 883
- Oosterloo, T., & van Gorkom, J., 2005, *A&A*, 437, L19
- Palunas, P., & Williams, T. B., *AJ*, 120, 2884
- Poggianti, B. M., et al. 1999, *ApJ*, 518, 576
- Poggianti, B. M., et al. 2001, *ApJ*, 562, 689
- Poggianti, B. M., et al. 2004, *ApJ*, 601, 197
- Popesso, P., Bohringer, H., Romaniello, M., & Vogas, W. 2005, *A&A*, 433, 415
- Popesso, P., Biviano, A., Bohringer, H., & Romaniello, M. 2006, *A&A*, 445, 29
- Postman, M., & Geller, M. J. 1984, *ApJ*, 281, 95
- Postman, M., et al. 2005, *ApJ*, 623, 721
- Quilis, V., Moore, B., & Bower, R. 2000, *Science*, 288, 1617
- Roediger, E., & Hensler, G. 2005, *A&A*, 433, 875
- Roediger, E., & Brüggen, M. 2007, *MNRAS*, 380, 1399
- Sakai, S., et al. 2002, *ApJ*, 578, 842
- Schlegel, D. J., Finkbeiner, D. P., & Davis, M. 1998, *ApJ*, 500, 525
- Schweizer, F. 1978, in *Structure and Properties of Nearby Galaxies*, p. 279
- Schulz, S., & Struck, C. 2001, *MNRAS*, 328, 185
- Smith, G. P., Treu, T., Ellis, R. S., Moran, S. M., & Dressler, A. 2005, *ApJ*, 620, 78
- Struck, C., & Brown, J. R. 2004, in *Duc, P.-A., Braine, J. & Brinks, E., eds., Recycling Intergalactic and Interstellar Matter*, IAU Symposium No. 217, p. 466
- Sun, M., Donahue, M., & Voit, M. 2007, *ApJ*, 671, 170
- Tran, H. D., et al. 2003, *ApJ*, 585, 750
- Trentham, N., Sampson, L., & Banerji, M. 2005, *MNRAS*, 357, 783
- van der Wel, A., et al. 2007, *ApJ*, 670, 206
- Vollmer, B., & Huchtmeier, W. 2003, *A&A*, 406, 427
- Vollmer, B., Cayatte, V., Balkowski, C., & Duschl, W. J. 2001, *ApJ*, 561, 708
- Vollmer, B., Beck, R., Kenney, J. D. P., & van Gorkom, J. H. 2004, *AJ*, 127, 3375
- Yagi, M., et al. 2007, *ApJ*, 660, 1209
- Yamanoi, H., et al. 2007, *AJ*, 134, 56
- Yoshida, M., et al. 2002, *ApJ*, 567, 118
- Yoshida, M., et al. 2004, *AJ*, 127, 90
- Yoshino, A., & Ichikawa, T. 2008, *PASJ*, 60, 493

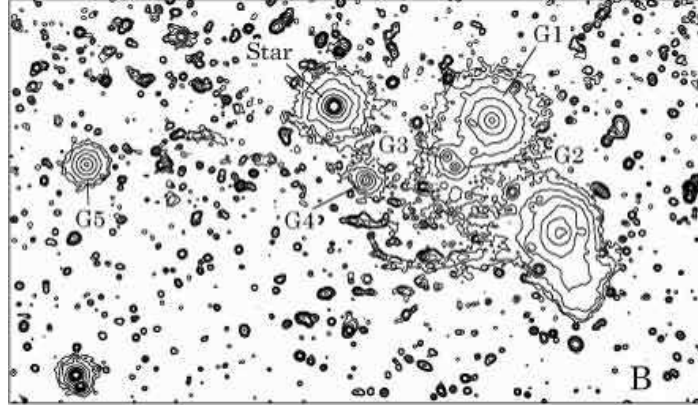


FIG. 2.— B contour map around RB199. The orientation is the same as Figure 1. To improve the signal-to-noise ratio of the faint features, the original images were smoothed by 4×4 pixels running mean to produce the contour maps in Figure 2 and Figure 3. The lowest contour level of this image is $28.5 \text{ (AB)mag arcsec}^{-2}$ and the contour interval is 1 mag. “G1”–“G5” are galaxies near RB199. The object lying to the east of the galaxy G4 is a foreground star.

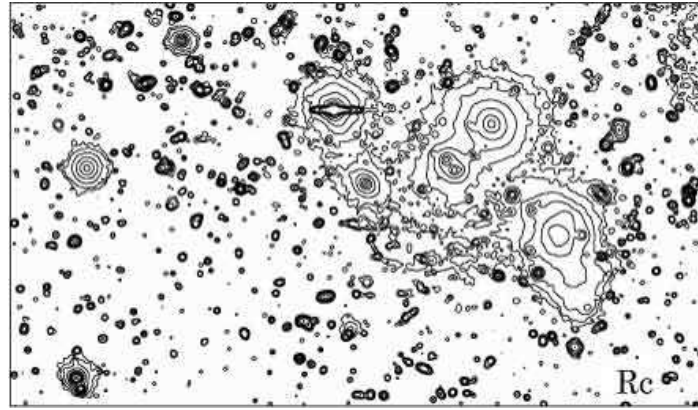


FIG. 3.— R_C contour map around RB199. The lowest contour level is $27.8 \text{ (AB)mag arcsec}^{-2}$ and the contour interval is 1 mag.

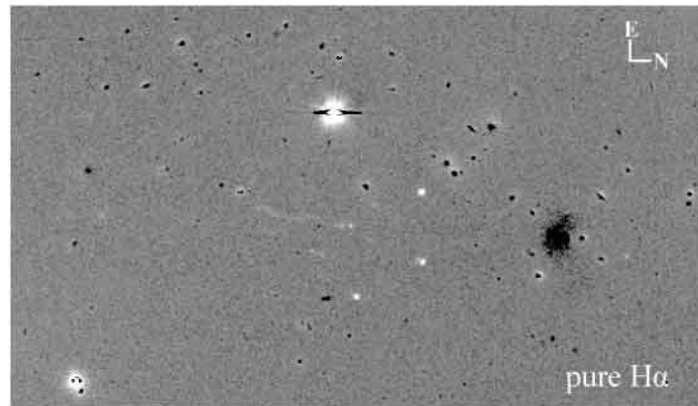


FIG. 4.— Continuum subtracted $H\alpha$ image around RB199. Stronger $H\alpha$ is coded whiter.

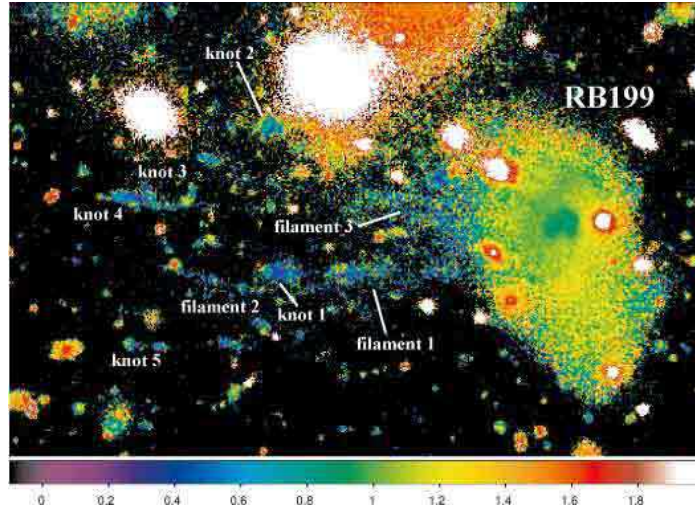


FIG. 5.— $B - R_C$ color map of the RB199 field. This map shows the $B - R_C$ color from 0.0 (violet) to 1.8 (red) (see the color bar at the bottom of the figure).

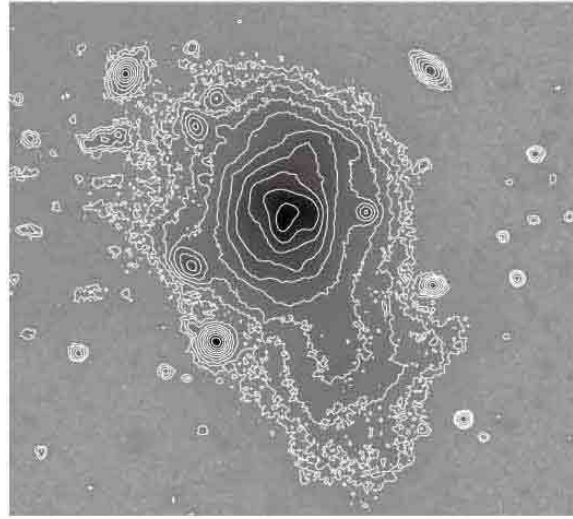


FIG. 6.— B band image of RB199 (contour map overlaid on the grayscale image). The lowest contour level and the contour interval are $26.5 \text{ (AB)mag arcsec}^{-2}$ and 0.5 mag , respectively.

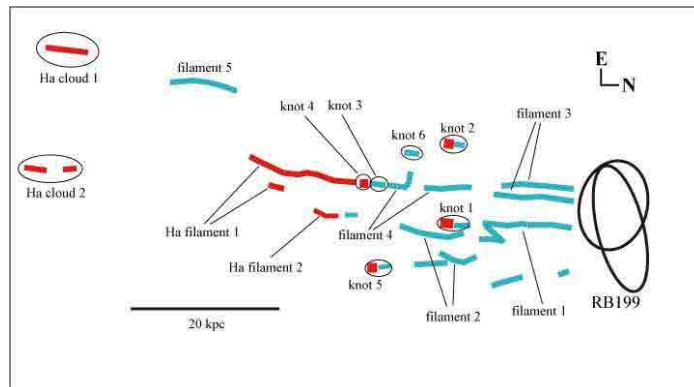


FIG. 7.— Schematic view of the “fireballs” of RB199.

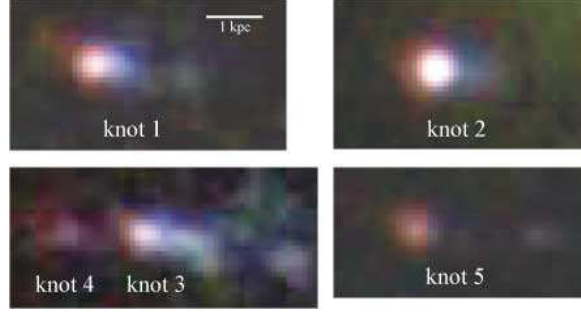


FIG. 8.— Close-up views of the bright knots. Enlarged false-color images of the knot 1 (upper left), the knot 2 (upper right), the knot 3 (lower left), and the knot 5 (lower right) are shown. The attribute of the color is the same as in Figure 1.

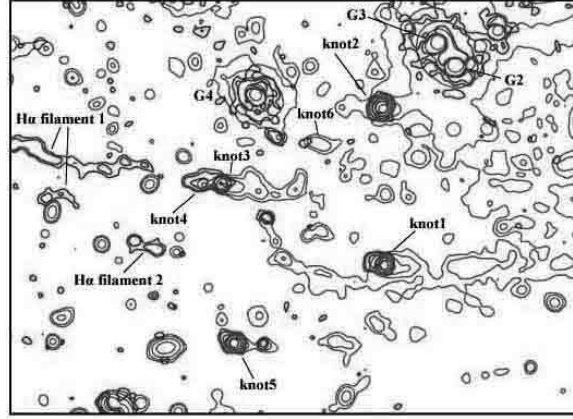


FIG. 9.— Contour map of the pure H α image (red lines) is overlaid on a contour map of the B image (blue lines). Lowest contour levels of the pure H α and the B maps are $2.4 \times 10^{-18} \text{ erg cm}^{-2} \text{ s}^{-1} \text{ arcsec}^{-2}$ and 28 (AB)mag arcsec $^{-2}$, respectively. Contour interval is 1 mag for both maps.

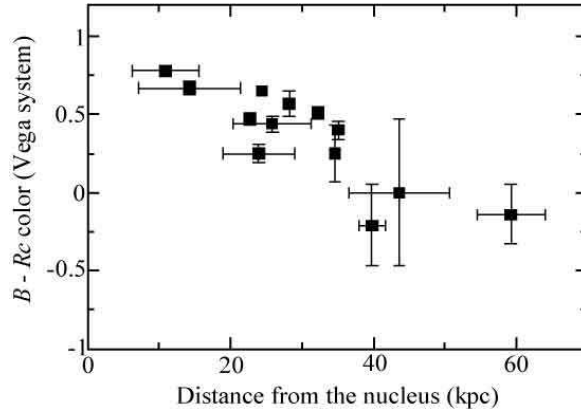


FIG. 10.— $B - R_C$ colors of the knots and filaments of the fireballs are shown with respect to the distance from the nucleus of RB199. The horizontal error bars indicate the length of the features.

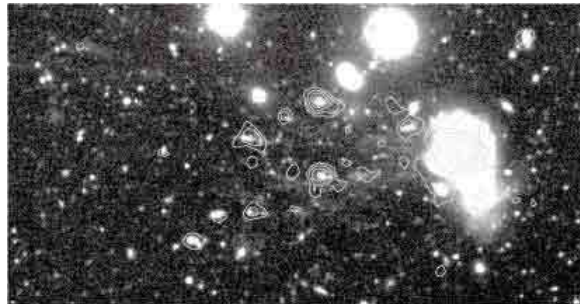


FIG. 11.— GALEX FUV contour map overlaid on the B band image of RB199.



FIG. 12.— GALEX NUV contours map overlaid on the B band image of RB199.

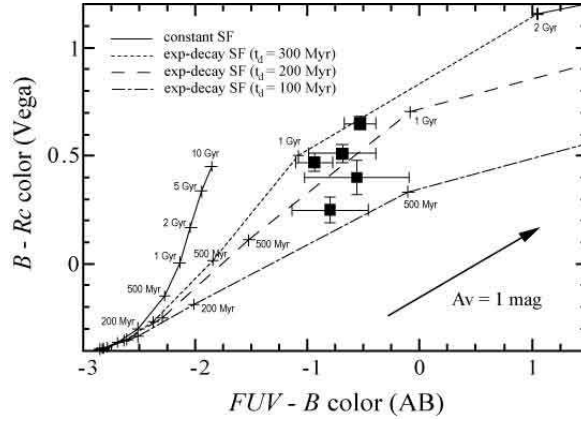


FIG. 13.— Color-color diagram of $B - R_C$ versus $FUV - B$ for the bright knots and the blue filaments of the fireballs. The black squares represent the knot colors. The solid lines are the model prediction for the constant star-formation case. The dot-dashed lines, the dashed lines, and the dotted lines are the predictions of exponential decaying star formation models with decay timescales of 100 Myr (E100 model), 200 Myr (E200 model), and 300 Myr (E300 model), respectively. The arrows show the effect of internal dust extinction on the observed colors.

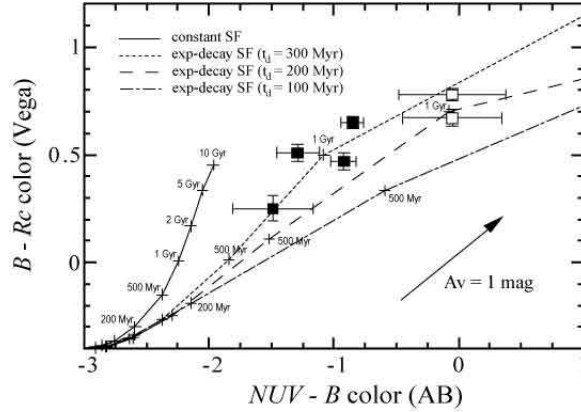


FIG. 14.— Color-color diagram of $B - R_C$ versus $NUV - B$ for the fireballs. The white squares represent the colors of filaments 1 and 3. The other symbols and lines are the same as in Figure 13.

TABLE 1
OBSERVATION LOG

| filter | PSF size | SB _{lim} (ABmag arcsec ⁻²) ^a | date (UT) | exposure |
|----------------------|----------|--|------------|--------------|
| <i>B</i> | 1".06 | 28.8 | 2006-04-28 | 2 × 450sec |
| | | | 2006-05-03 | 3 × 450sec |
| | | | 2007-05-13 | 5 × 600sec |
| <i>R_C</i> | 0".81 | 28.0 | 2006-04-28 | 11 × 300 sec |
| | | | 2007-05-14 | 5 × 360 sec |
| | | | 2007-05-15 | 1 × 300 sec |
| NB | 0".82 | 27.8 | 2006-04-28 | 5 × 1800 sec |
| | | | 2007-05-15 | 8 × 1800 sec |

^a SB_{lim} represent 1- σ fluctuation of a circular aperture of 2 arcsec diameter. The *R_C* and NB are calibrated by short exposures taken on 2006-05-03, but the mosaic image does not include them.

TABLE 2
PHOTOMETRY OF THE FIREBALLS AROUND RB199

| ID | distance ^a | size ^b | <i>m_B</i> | <i>m_{R_C}</i> | <i>B</i> − <i>R_C</i> | <i>M_L</i> ^c | <i>L_{Hα}</i> ^d | SFR ^e |
|-----------------------|-----------------------|-------------------|----------------------|----------------------------------|---------------------------------|-----------------------------------|--|------------------|
| knot 1 | 23 | 2.6×0.9 | 22.52±0.03 | 22.04±0.03 | 0.47±0.04 | 8.8 | 34 | 27 |
| knot 2 | 24 | 1.8×1.0 | 22.18±0.02 | 21.53±0.02 | 0.65±0.03 | 14 | 59 | 47 |
| knot 3 | 32 | 1.9×0.6 | 23.19±0.03 | 22.68±0.03 | 0.51±0.04 | 4.8 | 9.9 | 7.8 |
| knot 4 | 34 | 0.7×0.7 | 25.13±0.12 | 24.88±0.13 | 0.25±0.18 | 0.76 | 2.1 | 1.7 |
| knot 5 | 35 | 0.7×0.7 | 24.06±0.04 | 23.66±0.04 | 0.40±0.06 | 2.3 | 30 | 23 |
| knot 6 | 28 | 0.6×1.6 | 24.23±0.06 | 23.66±0.05 | 0.57±0.08 | 2.0 | 3.2 | 2.5 |
| filament 1 | 14 | 14 | 22.03±0.03 | 21.36±0.03 | 0.67±0.04 | 16 | - | - |
| filament 2 | 24 | 9 | 22.53±0.04 | 22.28±0.03 | 0.25±0.04 | 6.7 | 0.9 | 0.7 |
| filament 3 | 11 | 10 | 22.10±0.02 | 21.32±0.05 | 0.78±0.06 | 16 | - | - |
| filament 4 | 26 | 5 | 22.83±0.04 | 22.39±0.03 | 0.44±0.05 | 6.4 | 5.9 | 4.7 |
| filament 5 | 59 | 8 | 23.22±0.15 | 23.36±0.11 | -0.14±0.16 | 2.5 | 3.8 | 3.0 |
| H α filament 1 | 44 | 14 | 25.39±0.48 | 25.39±0.32 | 0.00±0.48 | 0.68 | 28 | 23 |
| H α filament 2 | 40 | 4 | 24.86±0.12 | 25.07±0.23 | -0.21±0.26 | 0.52 | 12 | 9.2 |
| H α cloud 1 | 80 | - | 26.04±0.25 | - | - | 0.62 ^f | 9.0 | 7.2 |
| H α cloud 2 | 79 | - | 26.29±0.62 | - | - | 0.50 ^f | 11 | 8.6 |
| Total | 83 ^g | | 19.87 | 19.33 | 0.54 | 110 | 225 | 179 |

^adistance from the nucleus of RB199 in units of kpc.

^bsizes of the knots, filaments, and cloud in units of kpc. The sizes are measured at the *B* band surface brightness of 28 mag arcsec⁻².

^cmass derived from *R_C* band magnitude in units of 10⁶ M_⊙ assuming that *M/L_R* = 1.

^dH α luminosity in unit of 10³⁷ ergs s⁻¹. Contamination of [NII] $\lambda\lambda$ 6548/6583 emission and internal dust extinction is not corrected.

^estar-formation rate calculated from *L_{H α}* in units of 10⁻⁴ M_⊙ yr⁻¹ assuming that all the H α emission is produced by star-formation activity.

^fderived from *B* band magnitude assuming that *M/L_B* = 1.

^gdistance between the edge of the H α cloud 1 and the nucleus of RB199.

TABLE 3
ULTRAVIOLET MAGNITUDES AND OPTICAL-UV COLORS OF THE FIREBALLS

| ID | GALEX ID | GALEX FUV ^a (AB mag) | GALEX NUV ^a (AB mag) | FUV − <i>B</i> (AB mag) | NUV − <i>B</i> (AB mag) |
|------------|--------------------|------------------------------------|------------------------------------|----------------------------|----------------------------|
| knot 1 | J125841.9 + 274451 | 21.44±0.16 | 21.46±0.09 | -0.94±0.16 | - 0.92±0.10 |
| knot 2 | J125843.8 + 274450 | 21.51±0.14 | 21.19±0.08 | -0.53±0.14 | - 0.85±0.09 |
| knot 3 + 4 | J125842.9 + 274427 | 22.36±0.30 | 21.76±0.17 | -0.69±0.30 | -1.29±0.21 |
| knot 5 | J125841.0 + 274429 | 23.12±0.34 | 22.43±0.33 ^b | - 0.80±0.34 | -1.49±0.33 |
| knot 6 | J125843.4 + 274439 | 23.53±0.45 | - | -0.56±0.46 | - |
| filament 1 | - | - | 21.84±0.40 ^b | - | - 0.19±0.40 |
| filament 3 | - | - | 21.91±0.43 ^b | - | - 0.19±0.43 |

^aTaken from the Web site of GALEX data release 2 (DR2), except for the NUV magnitudes of knot 5, filament 1, and filament 3.

^bDirectly measured in the NUV image calibrated by the GALEX DR2 NUV magnitude of knot 1.